



Scholars Research Library

Der Pharma Chemica, 2015, 7(10):260-274
(<http://derpharmachemica.com/archive.html>)



ISSN 0975-413X
CODEN (USA): PCHHAX

New antipyrine derivatives as corrosion inhibitors for C-steel in 1.0M hydrochloric acid solutions

A. S. Fouda*, G. Y. Elewady, R.R. Ibrahim and E. A. Salim

Chemistry Department, Faculty of Science, El -Mansoura University, El-Mansoura, Egypt

ABSTRACT

Adsorption and inhibition efficiency effect of antipyrine derivatives on the C-steel in 1.0M HCl were estimated using three electrochemical techniques (electrochemical impedance spectroscopy (EIS), electrochemical frequency modulation (EFM) and Potentiostatic polarization). Inhibition efficiency of the inhibitors rose with raising the concentration of the derivatives as well as increased also with rising the temperature. Polarization curves revealed that these compounds are chemical type inhibitors. The adsorption of these compounds follows Langmuir adsorption isotherm. Some thermodynamic parameters of activation and adsorption processes were also estimated and discussed.

Keywords: Corrosion inhibition, carbon steel, HCl, antipyrine derivatives.

INTRODUCTION

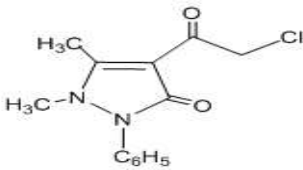
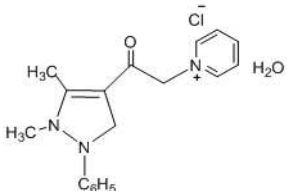
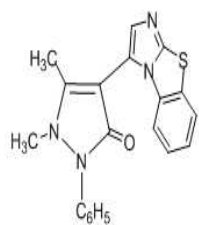
Corrosion is often essential method enjoying an important position inside economics. The usage of inhibitors is the most effective methods for defense in contrast to corrosion, particularly in acidic medium [2]. Organic materials are considered to be the most effective inhibitors involving nitrogen, sulfur, and oxygen atoms. Among them, organic inhibitors have various benefits such as high inhibition efficiency, low cost, low toxicity, and easily produced [3-6]. Organic heterocyclic materials were used for the corrosion inhibition of iron [7-12], copper [13], aluminum [14-16], and other metals [17-18] in various corroding media. The adsorption of the surfactant heterocyclic inhibitors on the metal surface can obviously change the corrosion-resisting property of the metal [19-20], so studying of the relations between the adsorption and corrosion inhibition is of huge relevance. Heterocyclic compounds have shown high inhibition efficiency for iron in both HCl [21] and H₂SO₄ [22] solutions. As antipyrine compounds have been studied as corrosion inhibitors before we also used some derivatives of it to inhibit corrosion of C-steel in 1M HCl. For this reason, the goal of the present work is to investigate the inhibiting action of antipyrine derivatives in 1M HCl at 25-45 °C using different methods.

MATERIALS AND METHODS

The electrode which we used in experiments was made from C-steel sheets. Before every experiment, the electrode which we use was refined with emery paper of several grades up to 1000 grit, dipped by acetone and lastly by bi-distilled water.

Experiments were conducted in 1M HCl solution with different concentrations ($3 \times 10^{-6} \text{M} - 18 \times 10^{-6} \text{M}$) of antipyrine compounds. The structures and molecular weights of the investigated antipyrine compounds are shown in table (1) [1]. All solutions were freshly prepared using analytical grade reagents and bi-distilled water. All experiments were performed at required temperature $\pm 1^\circ\text{C}$.

Table 1: Structures, names, chemical formulas and molecular weights of the investigated antipyrine derivatives

No	Structures and names	Chemical formulas	Mol.Weights
1	<p>4-2(chloroacetyl)-1,5-dimethyl-2-diphenyl-1H-pyrazol-3(2H)-one</p> 	$C_{13}H_{13}ClN_2O_2$	264.71
2	<p>1-(2(1,5dimethyl-2-phenyl-2,3-dihydro-1H-pyrazol-4-yl)-2-oxoethyl)pyridiniumchloride hydrate</p> 	$C_{18}H_{22}ClN_3O_2$	347.87
3	<p>2-aminobenzimidazole</p> 	$C_{20}H_{16}N_4OS$	360.43

RESULTS AND DISCUSSION

1. Polarization measurements

Polarization experiments were being accomplished in three-electrode cell with a platinum counter electrode as well as a saturated calomel electrode (SCE) coupled to a fine Luggin capillary that acts as reference electrode. The operating electrode was cut squarely from C-steel embedded in epoxy resin of polytetrafluoroethylene (PTFE) so that the flat surface was the only surface of the electrode. The working surface area was $1.0 \times 1.0 \text{ cm}$. Polarization technique was carried out with an automatically potential from -500 to $+500 \text{ mV}$ at open circuit potential with a scan rate of 1 mVs^{-1} . Stern-Geary method [23] applied extrapolation of anodic and cathodic Tafel lines were plotted to investigate the corrosion current, also getting $\log i_{\text{corr}}$ as well as the analogous corrosion potential (E_{corr}) for inhibitor free acid and for every inhibitor concentration. i_{corr} was utilized for estimation of efficiency of inhibition and surface coverage (θ) as below:

$$IE \% = \theta \times 100 = [1 - (i_{\text{corr(inh)}} / i_{\text{corr(free)}})] \times 100 \quad (2)$$

where $i_{\text{corr(free)}}$ and $i_{\text{corr(inh)}}$ are the densities of corrosion current without and with of inhibitor, in that order.

The frequency range used for impedance measurements from 100 kHz to 10 mHz with amplitude of 5 mV peak-to-peak via ac signals at open circuit potential. Basic parameters calculated from the analysis of Nyquist graph are the resistance of charge transfer R_{ct} (diameter of high frequency loop) and the capacity of double layer C_{dl} that is defined as:

$$C_{dl} = 1 / (2 \pi f_{max} R_{ct}) \quad (3)$$

where f_{max} is the maximum frequency

The efficiencies of inhibition and the surface coverage (θ) attained from the impedance determinations were defined by this equation:

$$IE \% = \theta \times 100 = [1 - (R_{ct}^0 / R_{ct})] \times 100 \quad (4)$$

where R_{ct}^0 and R_{ct} are the charge transfer resistance with out and with inhibitor, in that order. 30 min was the time allowed for the electrode potential to stand before beginning the measurements. Experiments were performed at $25 \pm 1^\circ\text{C}$. Gamry (PCI 300/4) Instrument Potentiostat/Galvanostat/ZRA was used to calculate the measurements. This contains a Gamry framework system mainly based on the ESA 400. Gamry applications involve DC105 for corrosion determinations and EIS300 for electrochemical impedance spectroscopy with a computer for obtaining data; finally we used Echem Analyst 5.58 software.

We noticed from the diagram that the negative shift of corrosion potential suggests that the applied materials are chemical type inhibitors but mainly cathodic inhibitor than anodic one. From the list of data below we can see that the diminish in density of corrosion current and the raising in efficiency of inhibition is due to the adsorption of the applied inhibitors on C-steel. The following diagram shows the highest inhibitor (compound 3) in inhibition process. The other inhibitors were investigated but not shown. Table 2 shows the data obtained for all inhibitors.

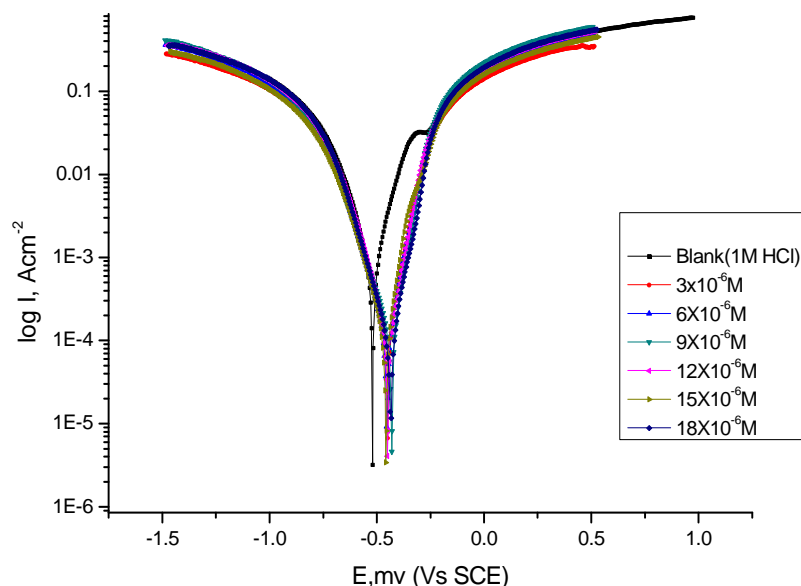


Figure (1) Potentiostatic polarization diagrams for dissolution of C-steel in 1.0M HCl without and with different concentrations of inhibitor (3) at 30°C

Table (2) shows the potentiostatic polarization parameters for all compounds

Inhibitor	[Inh] M x10 ⁶	-E _{corr.} , mV vs SCE	i _{corr.} , μA cm ⁻²	β _a , mV dec ⁻¹	β _c , mV dec ⁻¹	C.R. mpy	Θ	% IE
Blank	0	520	668	93	113	305.2	----	----
1	3	512	578	90	115	264	0.135	13.4
	6	515	438	83	111	200.1	0.344	34.4
	9	511	411	78	115	187.9	0.385	38.5
	12	505	348	83	126	159.1	0.480	47.9
	15	500	336	73	116	153.6	0.497	49.7
	18	458	238	107	127	108.9	0.644	64.4
2	3	450	130	81	120	59.6	0.805	80.5
	6	452	128	86	120	58.6	0.808	80.8
	9	450	125	82	106	57.0	0.813	81.2
	12	431	125	76	135	56.9	0.813	81.3
	15	458	107	68	109	48.7	0.839	83.9
	18	436	106	83	117	48.5	0.841	84.1
3	3	563	233	565	146	106.6	0.651	65.1
	6	575	209	599	147	95.7	0.687	68.7
	9	483	133	160	126	60.9	0.800	80
	12	545	93.2	199	85	42.6	0.860	86
	15	494	68.1	129	113	31.1	0.898	89.8
	18	544	28.7	120	159	13.1	0.957	95.7

2. Electrochemical frequency modulation measurements

The EFM method is used to estimate the slopes of anodic and cathodic Tafel, also the densities of corrosion current for the investigated compound. Figure (2) shows the EFM intermodulation spectra (spectra of current response as a function of frequency) of C-steel in 1.0 M HCl. The measured electrochemical parameters (i_{corr.}, β_c, β_a, CF-2, CF-3 and %IE) are given in Table (3). From the Table we can observe that the corrosion current density decreases with raising the concentration of the studied compounds with respect to blank and hence the inhibition efficiency increases and reveal that the investigated compounds inhibit the acid corrosion of C-steel through adsorption[24].

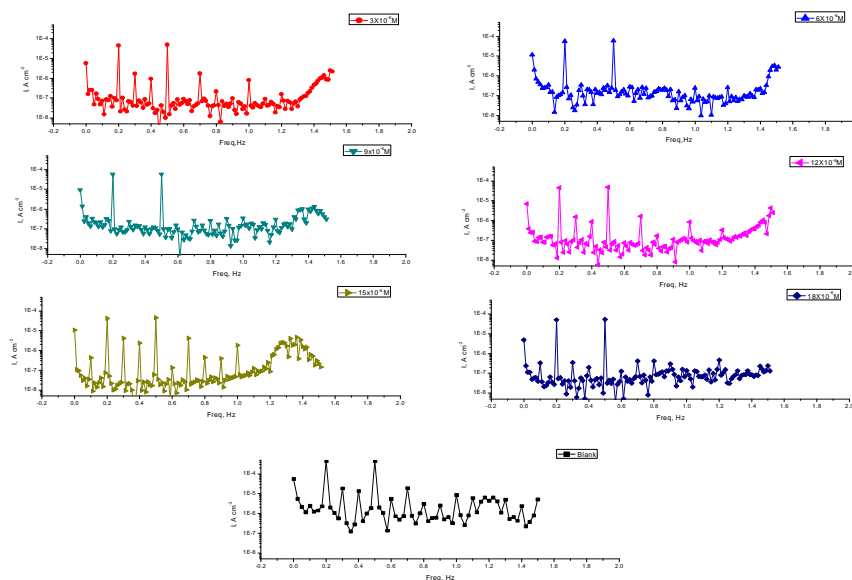


Figure (2) EFM spectra of C-steel in 1.0M HCl for inhibitor(3) at 30°C

Table3: shows the electrochemical frequency modulation parameters for investigated compounds

Inhibitor	[inh] M x10 ⁶	i_{corr} μAcm^{-2}	β_a mVdec^{-1}	β_c mVdec^{-1}	CF-2	CF-3	C.R mpy	Θ	% IE
Blank	0	1009	122	180	1.714	-	461	-	-
1	3	628.1	98	126	1.94	2.778	287	0.377	37.7
	6	542.9	88	113	2.078	2.825	248.1	0.461	46.2
	9	477	78	91	1.887	3.75	218	0.527	52.7
	12	408.8	85	119	1.96	2.853	186.8	0.594	59.5
	15	400.8	90	125	2.008	2.265	183.1	0.602	60.3
	18	394.9	47	55	1.399	1.337	180.4	0.608	60.8
2	3	282.6	81	138	1.973	2.885	129.1	0.719	71.9
	6	267.9	75	115	1.923	3.565	122.4	0.734	73.4
	9	263	77	117	1.964	2.822	120.2	0.739	73.9
	12	253	82	140	1.915	2.927	115.6	0.749	74.9
	15	221.6	77	144	1.96	2.764	101.3	0.78	78
	18	190.1	72	130	1.874	3.795	86.8	0.811	81.2
3	3	173.1	189	327	1.97	-	79.0	0.828	82.8
	6	161.7	176	185	1.528	-	73.8	0.839	83.9
	9	150.2	164	171	1.066	1.062	68.6	0.851	85.1
	12	148.8	169	257	1.856	-	68	0.852	85.2
	15	114.1	115	348	1.956	1.91	52.1	0.886	88.7
	18	109.6	131	139	2.287	2.098	50.0	0.891	89.1

3. Electrochemical impedance spectroscopy measurements

The inhibitor concentration effect on the impedance action of C-steel in 1.0 M HCl solution at 25 °C is obtainable in Fig. (3). Nyquist diagrams for C-steel in the presence of different concentrations of inhibitor (3) were plotted. The presence of single semi-circle revealed the single charge transfer process throughout dissolution that is not affected by the existence of inhibitor particles. Deviations from the circular shape are related to the frequency dispersion of interfacial impedance according to surface roughness, dislocations, impurities, adsorption of inhibitors, grain boundaries, and formation of porous layers and in homogenates of the electrode surface [25]. The highest inhibitor (inhibitor 3) in inhibition is shown in Fig. 3. The others are not shown but data for all compounds are listed in Table 4.

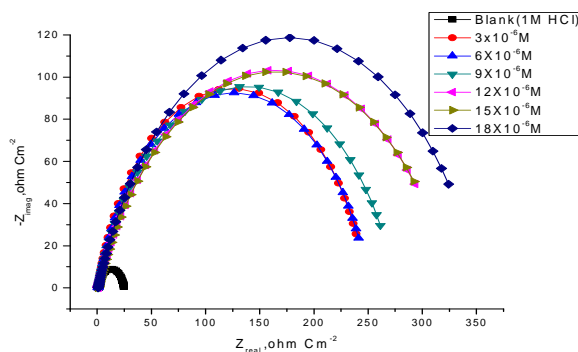


Figure (3a) Nyquist curves for corrosion of C-steel in 1.0 M HCl with out and with various concentrations of inhibitor (3) at 25°C

Variables of electrochemical kinetic obtained by EIS method for the corrosion of C-steel in 1.0M HCl at various concentrations of investigated compounds at 25°C were reported in Table (4). It is clear from the Table that the polarization resistance raises with raising the tested compounds concentration while C_{dl} values tend to reduce. The reduce in C_{dl} is owing to the adsorption of the tested compounds on C-steel surface [26] and it can be explained on the basis that the double layer between charged C-steel surface and solutions considered as an electrical capacitor. The decrease in the capacitance could be due to the protective layer formation on C-steel surface [27].

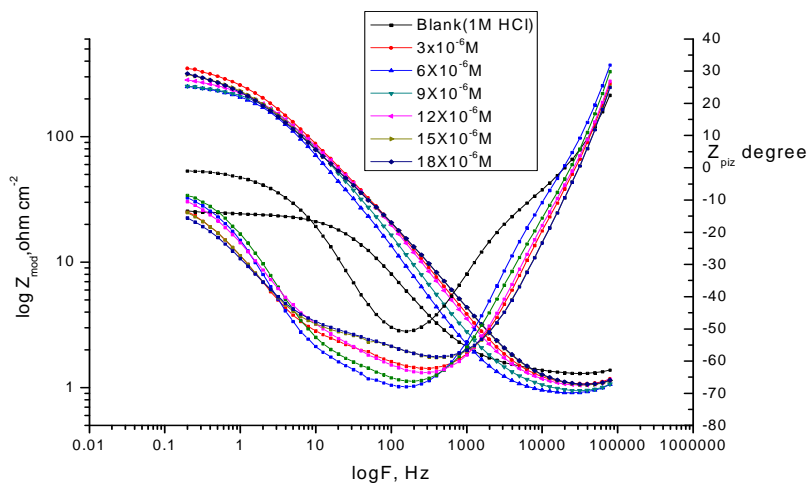


Figure (3b) The Bode diagram for corrosion of steel in 1.0 M HCl with out and with various concentrations of inhibitor (3) at 25°C

Table(4): Electrochemical kinetics results obtained by EIS technique for the three inhibitors in 1.0M HCl at 25°C

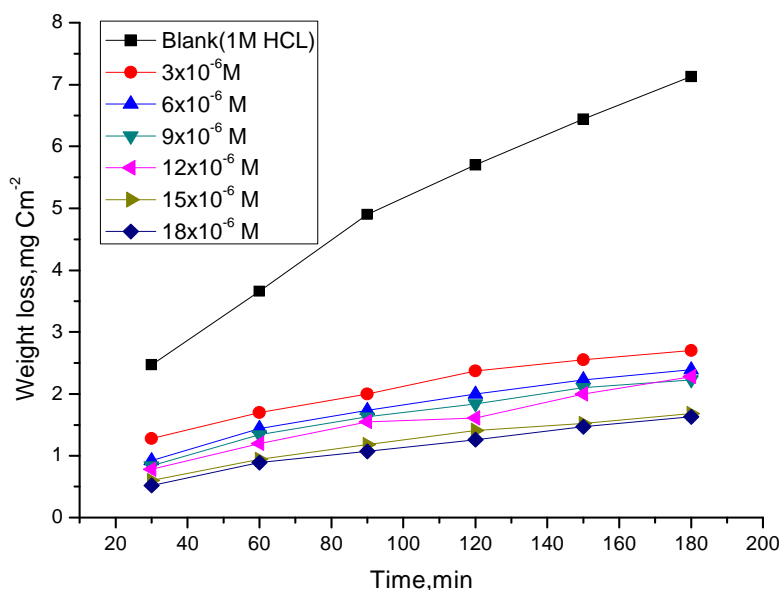
Inhibitor	[inh] M x10 ⁶	R _{ct} , Ω cm ²	R _s , Ω cm ²	C _{dl} , *10 ⁻⁴ Fcm ⁻²	Θ	% IE
Blank	0	23.5	1.323	2.349	-----	-----
1	3	28.4	1.111	1.264	0.173	17.3
	6	28.6	1.193	2.582	0.178	17.8
	9	33.9	1.724	2.213	0.307	30.7
	12	35.4	1.53	1.945	0.335	33.5
	15	49.6	1.281	2.457	0.525	52.5
	18	53.4	1.193	2.135	0.559	55.9
2	3	66.5	1.426	2.184	0.646	64.6
	6	68.3	1.141	2.282	0.655	65.5
	9	72.4	1.999	2.478	0.674	67.4
	12	82.5	1.293	2.900	0.714	71.4
	15	101.3	1.276	3.047	0.767	76.7
	18	112.6	1.588	3.239	0.791	79.1
3	3	248.1	0.870	2.378	0.905	90.5
	6	250.1	0.905	2.003	0.905	90.5
	9	275.3	0.951	2.009	0.914	91.4
	12	326.6	0.910	2.647	0.927	92.7
	15	327.4	0.913	2.732	0.928	92.8
	18	352.4	0.958	2.250	0.933	93.3

4. Mass loss tests

Mass loss time graphs of steel with the adding of inhibitor (3) in 1.0M HCl at different concentrations is presented in Figure (4). The diagram of Figure (4) indicates that the mass loss values of steel in 1.0M HCl solution including investigated inhibitor diminish with the increase of inhibitors concentration, the curves of other inhibitors are not shown but data listed in Table (5).As the inhibitor concentration increases the inhibition efficiency increases. This kind of consequence comes from the fact that the adsorption of inhibitor on the steel raises with the inhibitor concentration, therefore steel surface is proficiently separated from the media by the creation of a film on its surface[25-28].Other figures and tables for inhibitors at different temperatures are not shown. Figure (4b) shows the effect of temperature

Table(5)Inhibition efficiency (%IE) of investigated inhibitors with various concentrations at 25°C from mass loss measurements at 120 min dipping in 1.0M HCl

[Inh]x10 ⁶ M	1		2		3	
	%IE	C.R.	%IE	C.R.	%IE	C.R.
3	6.5	0.039	17.3	0.041	58.4	0.018
6	14.0	0.034	25.0	0.035	64.9	0.016
9	25.9	0.030	35.7	0.031	67.7	0.015
12	43.6	0.027	42.0	0.027	71.7	0.013
15	50.4	0.023	50.2	0.023	75.3	0.010
18	55.4	0.020	55.2	0.021	77.8	0.010



Figure(4)Mass - loss time diagrams for C-steel with out and with various concentrations of inhibitor(3) at 25° C

Adsorption isotherms

It is largely identified that adsorption isotherm give useful information but the mechanism of the corrosion inhibition and the interaction between the adsorbed molecules themselves and their interaction with the electrode surface [29].The protection efficiency has often been taken as a measure of the degree of surface coverage of the metal surface with particular inhibitor. With this definition, the degree of surface coverage (θ) can be calculated from Eq. (3):

$$\theta = \% IE / 100(3)$$

The dependence of θ on inhibitor concentration (C) can be analyzed using Langmuir isotherm:

$$C/\theta=(1/K_{ads})+C(4)$$

where K_{ads} is the equilibrium constant of the adsorption reaction which related to standard free energy of adsorption ΔG°_{ads} by Eq. (5) [30]:

$$\log K_{ads} = -\log 55.5 - \Delta G^\circ_{ads} / 2.303RT(5)$$

where the value of 55.5 is the concentration of water in solution in mole /L. Hence, a plot of C/ θ versus C as shown in Figure (5), give a straight line with a slope of approximately equal unity and intercept equal 1/ K_{ads} . From slope and intercept we can calculate the equilibrium constant of adsorption K_{ads} . The heat of adsorption ΔH°_{ads} might be estimated by Van't Hoff equation [31]:

$$\log K_{\text{ads}} = \text{constant} - \Delta H_{\text{ads}}^{\circ}/2.303RT \quad (6)$$

In order to estimate adsorption heat ($\Delta H_{\text{ads}}^{\circ}$), $\log K_{\text{ads}}$ was plotted vs $1000/T$ as presented in Figure (6). The straightlines were obtained with slope equal to $(-\Delta H_{\text{ads}}^{\circ}/2.303R)$. Then according to this equation (7):

$$\Delta G_{\text{ads}}^{\circ} = \Delta H_{\text{ads}}^{\circ} - T\Delta S_{\text{ads}}^{\circ} \quad (7)$$

By calculating the obtained $\Delta G_{\text{ads}}^{\circ}$ and $\Delta H_{\text{ads}}^{\circ}$ values in eq. (7), the adsorption ($\Delta S_{\text{ads}}^{\circ}$) entropy values were estimated at all investigated temperatures. All estimated thermodynamic adsorption variables for studied compound on C-steel in 1.0M HCl solution were listed in Table (6). From the listed data it can be conclude that:

a) K_{ads} values increase with increasing the temperature from 25 –45°C

b) The negative sign of $\Delta G_{\text{ads}}^{\circ}$ indicate that the adsorption of the investigated compounds on C-steel surface is spontaneous process [32].

c) $\Delta G_{\text{ads}}^{\circ}$ may increase (become more negative) with an increase of temperature which indicates that the adsorption was favorable with increasing reaction temperature as the result of the inhibitor adsorption on metal surface [33].

d) It is usually accepted that the values of $\Delta G_{\text{ads}}^{\circ}$ around -20 kJ mol^{-1} or lower indicates the electrostatic interaction between charged metal surface and charged organic molecules in the bulk of the solution while those around -40 kJ mol^{-1} or higher involve charge charring or charge transfer between the charged metal and the organic molecules [35]. From the obtained values of $\Delta G_{\text{ads}}^{\circ}$ it was found that the existence of comprehensive adsorption (physical and chemical adsorption). That is to say, since the adsorption heat approached the general chemical reaction heat, the chemical adsorption occurs.

e) The negative sign of $\Delta H_{\text{ads}}^{\circ}$ reveals that the adsorption of the inhibitor molecules is an exothermic process. Generally, an exothermic adsorption process suggests either physisorption or chemisorption while endothermic process is attributed to chemisorption [34]. In an exothermic process, physisorption is compared to chemisorption by considering the absolute value of adsorption enthalpy. Generally, enthalpy values up to 41.9 kJ mol^{-1} are related to the electrostatic interactions between charged molecules and charged metal (physisorption) while those around 100 kJ mol^{-1} or higher are attributed to chemisorption. The unshared electron pairs in the investigated molecules may interact with orbitals of the metal to provide a protective chemisorbed film [35]. In the investigated compound the absolute values of $\Delta S_{\text{ads}}^{\circ}$ are relatively high, approaching those typical of chemisorption. The values of $\Delta S_{\text{ads}}^{\circ}$ in the presence of the investigated compounds are larger and negative values that are endothermic adsorption process [36].

Table (6) Thermodynamic variables for adsorption of inhibitors on steel surface in 1.0 M HCl at various temperatures

Inhibitor	Temperature C ⁰	$K_{\text{ads}} \times 10^{-3}$ M ⁻¹	$-\Delta G_{\text{ads}}^{\circ}$ kJ mol ⁻¹	$-\Delta H_{\text{ads}}^{\circ}$ kJ mol ⁻¹	$-\Delta S_{\text{ads}}^{\circ}$ J mol ⁻¹ K ⁻¹
1	25	62.1	37.3	22.8	201.819
	30	74.9	38.4		202.121
	35	62.1	38.6		199.330
	40	102.5	40.5		202.325
	45	109.1	41.3		201.685
2	25	48.5	36.7	30.9	226.786
	30	57.3	37.7		226.467
	35	68.9	38.8		226.342
	40	85.8	40.0		226.563
	45	105.5	41.2		226.727
3	25	488.9	42.4	34.1	256.784
	30	564.7	43.5		256.095
	35	604.8	44.4		254.837
	40	840.8	45.9		255.807
	45	1175.5	47.6		256.881

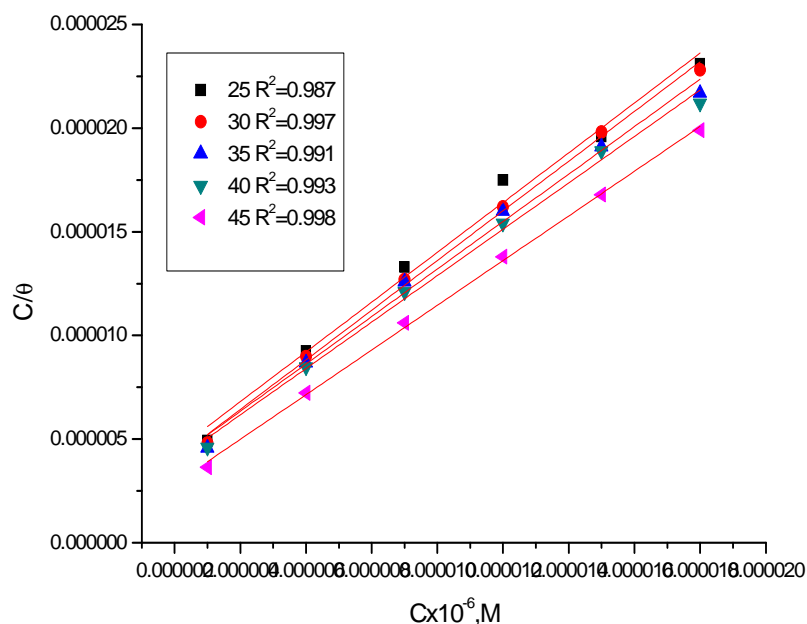


Figure (5) Langmuir adsorption isotherm of inhibitor (3) on C-steel surface in 1.0 M HCl at various temperatures

Effect of temperature

The effect of temperature on the corrosion rate of C-steel was investigated in 1.0M HCl solution in absence and presence of different concentrations of the investigated compounds in the temperature range 25–45°C. The values of corrosion parameters at different temperatures were calculated from electrochemical frequency modulation data. In general, the corrosion rate which is represented by the corrosion current density i_{corr} which increase with increasing temperature and the process obey to the familiar Arrhenius equation [37-38].

$$\log i_{\text{corr}} = \log A - E_a^*/2.303RT \quad (8)$$

where A is the pre-exponential factor, E_a^* is the apparent activation energy of the process and R is the universal gas constant. A plot of $\log i_{\text{corr}}$ versus $1000/T$ gave a straight line shown in Figure (7) with a slope equal $-E_a^*/2.303R$. The enthalpy of activation (ΔH^*) and the activation entropy (ΔS^*) were obtained by applying the transition state equation [39].

$$\log (i_{\text{corr}}/T) = \log (R/Nh) + (\Delta S^*/2.303R) - \log (\Delta H^*/2.303RT) \quad (9)$$

By plotting $\log (j_{\text{corr}}/T)$ versus $1/T$ gave a straight line shown in Fig (4d) with a slope $\Delta H^*/R$ and intercept $[\log (R/Nh) + \Delta S^*/2.303R]$. All estimated thermodynamic activation variables were listed in Table (7). It could be shown from the obtained data the presence of the investigated compounds lead to increase the activation energy to a value larger than that of uninhibited solution indicating that the higher energy barrier for the corrosion process in inhibited solution associated with chemical adsorption on C-steel surface [40]. All values of E_a^* are larger than the analogous values of ΔH^* indicating that the corrosion process must involve a gaseous reaction, simply the hydrogen evolution reaction [41]. The activation entropy ΔS^* in absence and presence of inhibitor has negative signs this suggests that the activated complex in the rate determining step prefer association rather than dissociation, meaning that, diminish in disordering takes place on going from reactants to the activated complex [42].

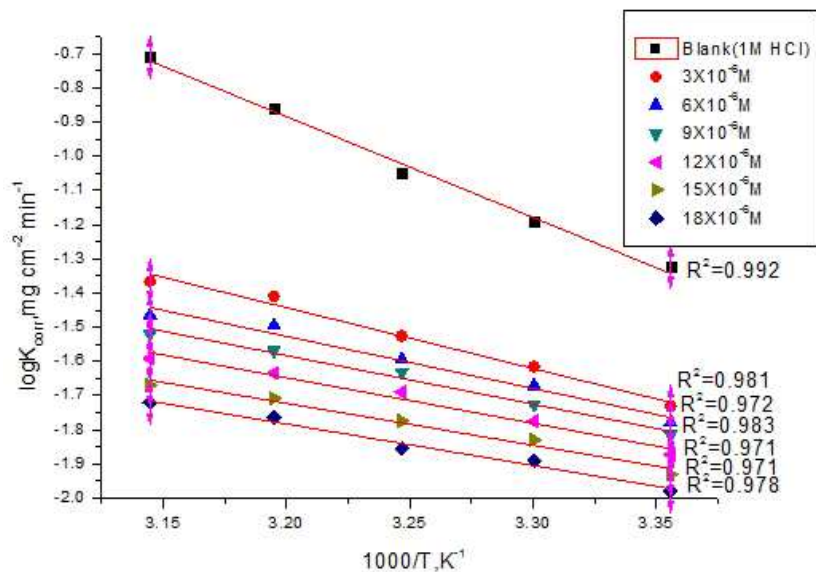


Figure (7) Arrhenius diagrams for carbon steel corrosion rates in 1.0M HCl in absence and presence of various doses of inhibitor (3)

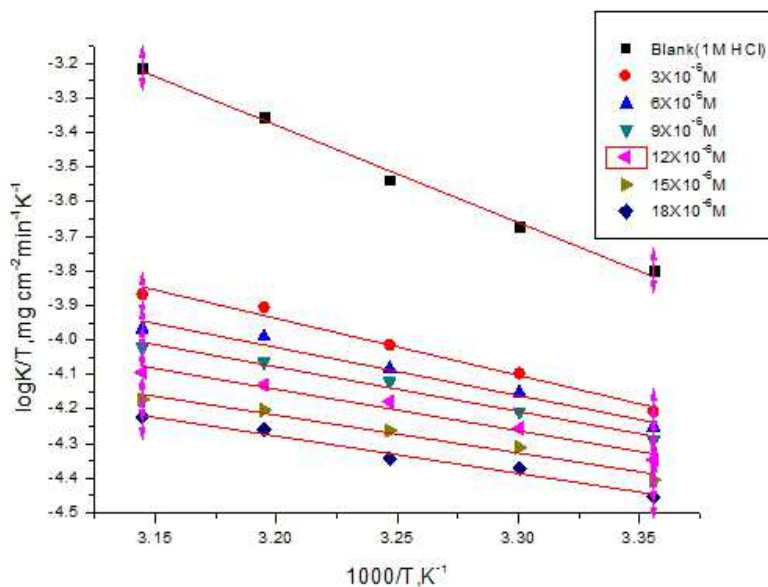


Figure (8) Transition diagrams for carbon-steel in 1.0M HCl in absence and presence of various doses of inhibitor (3).

5. Surface morphology

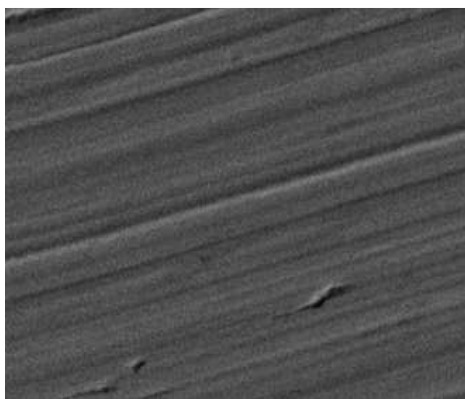
Scanning electron microscopy (SEM) and energy dispersive X-ray(EDX) examinations are carried out for the blank and the applied inhibitors and from these images we notice that the C-steel surface looks like not affected by corrosion. This because of the applied compounds is adsorbed on the C-steel surface by making protective film on the metal surface .This film is responsible for the highly efficient inhibition by these compounds. From Table 8 we can notice the lower values of Fe_{in} compound 3 < compound 2 < compound 1 and the amount of carbon on compound 3 > compound 2 > compound 1. This is in agreement of the %IE.

Table (7) Activation results for adsorption of inhibitors on carbon-steel in 1.0M HCl with out and with various concentrations of inhibitors

Inhibitor	[inh] x10 ⁶ M	E _a [*] kJ mol ⁻¹	ΔH [*] kJ mol ⁻¹	-ΔS [*] J mol ⁻¹ K ⁻¹
Blank	0	56.5	23.4	89.5
1	3	51.7	21.3	107.4
	6	48.6	20.0	118.7
	9	46.5	19.1	126.9
	12	42.9	17.5	140.2
	15	41.8	17.1	144.8
	18	40.6	16.5	149.7
2	3	49.9	21.7	104.1
	6	47.3	20.5	114.3
	9	44.9	19.5	123.1
	12	40.1	17.4	140.6
	15	35.7	15.5	156.4
	18	31.6	13.7	171.0
3	3	34.1	13.7	172.1
	6	29.2	11.6	189.4
	9	27.2	10.7	196.7
	12	25.5	9.9	203.4
	15	23.7	9.1	211.4
	18	23.3	8.9	213.2

Table (8) represents the data of EDX

(Mass %)	Fe	Mn	C	O
carbon steel alone	96.78	0.66	2.56	--
Blank	82.06	0.74	2.34	--
Inhibitor 1	82.84	0.77	11.45	3.5
Inhibitor 2	79.5	0.62	11.20	8.5
Inhibitor 3	78.1	0.70	16.85	4.5



Pure sample(a)

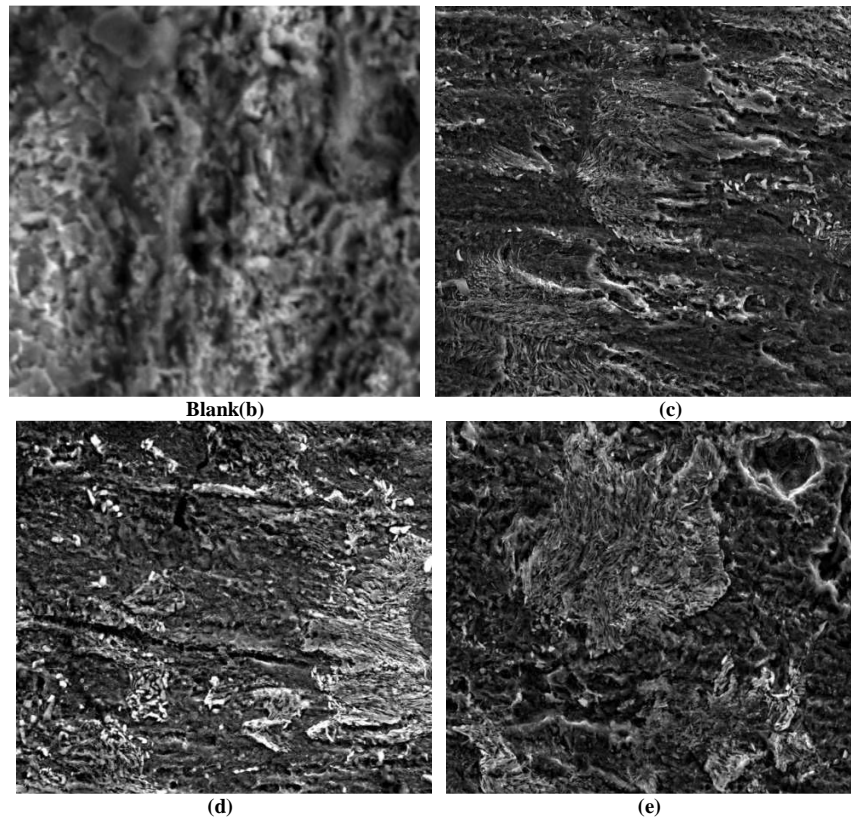
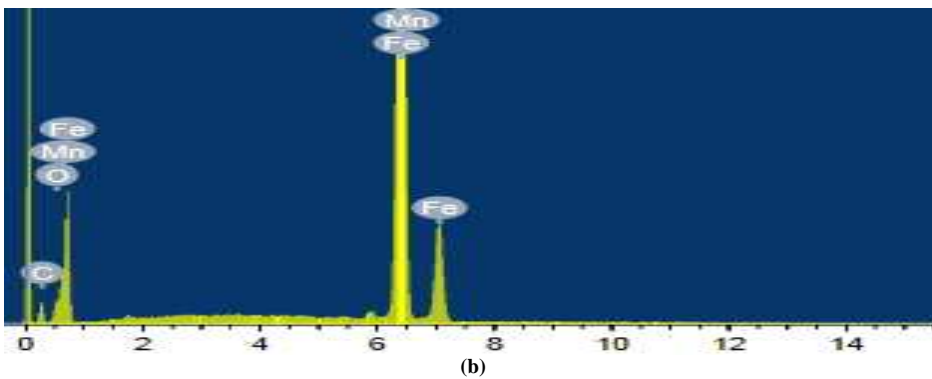
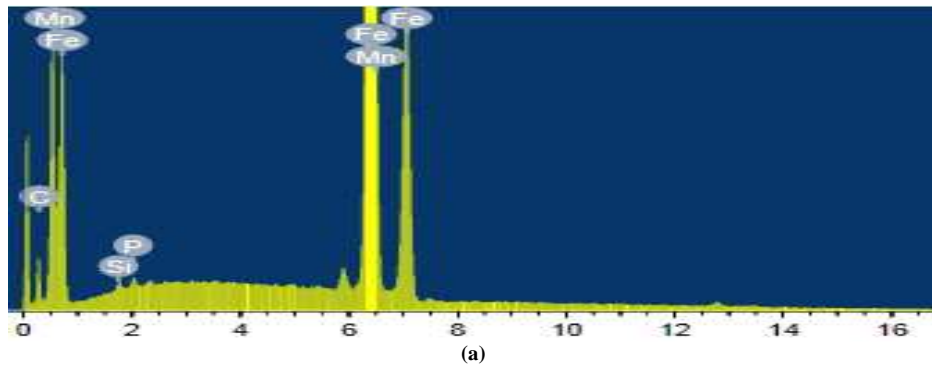


Figure (9) SEM images of C-steel surface in pure case (a) then after dipping in 1.0 M HCl only then (b) after 12h of dipping for inhibitor(1) (c), after 12h of dipping for inhibitor (2) (d) and after 12h of immersion for inhibitor(3)(e)



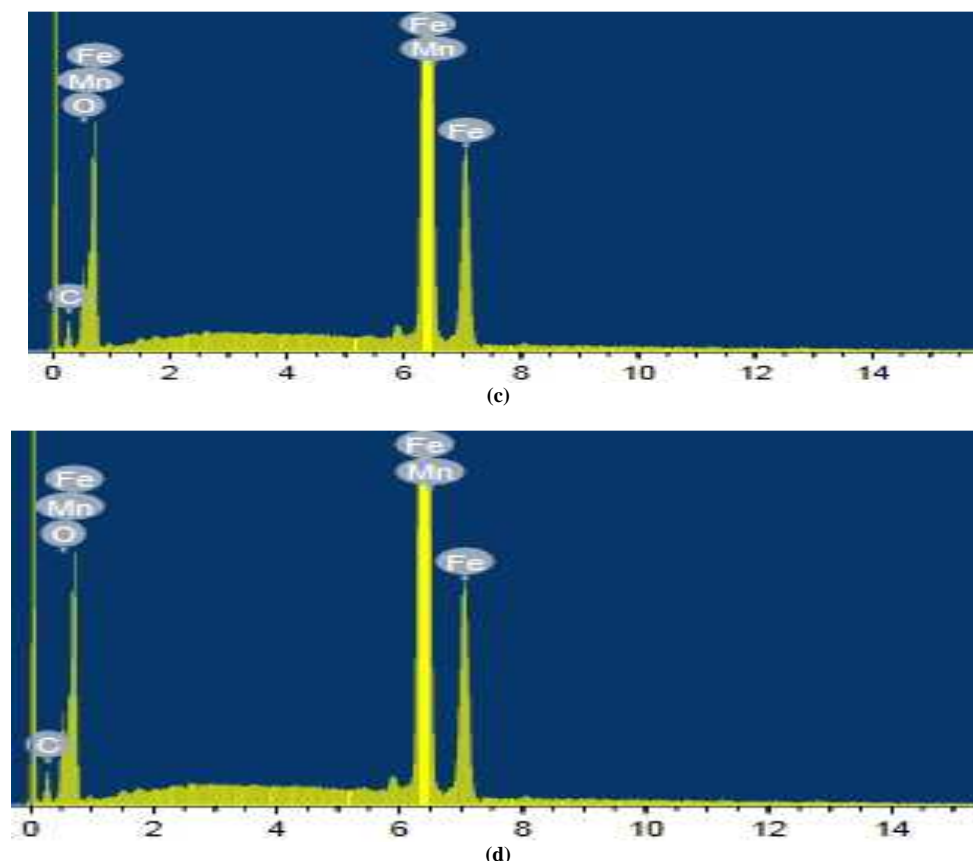


Figure (10) EDX spectra of C-steel in 1.0 M HCl blank (a) and in existence of (18×10^{-6} M) of inhibitor (1) (b), (18×10^{-6} M) of inhibitor(2), (c) (18×10^{-6} M) of inhibitor(3)(d)

Mechanism of inhibition

Corrosion inhibition of C-steel in HCl solution by the investigated compounds indicated from weight loss, potentiodynamic polarization, electrochemical impedance spectroscopy and electrochemical frequency modulation techniques was found to be depending on the concentration and nature of the investigated compounds. It is commonly, assumed that the inhibitor adsorption on the metal / solution interface is the initial step in the mechanism of the inhibitor in acid medium. Four kinds of adsorption might take place throughout inhibition involving organic molecules at the metal / solution interface 1) Electrostatic attraction among charged molecules and charged metal 2) interaction of unshared pairs of electrons in the molecule with the metal 3) Interaction of π electrons with the metal 4) A combination of the above [43]. Concerning inhibitors, the inhibition efficiency depend on numerous factors; for example (i) The adsorption sites number and their charge density, (ii) molecular size, (iii) mode of interaction with the metal surface and (iv) the formation of metallic complex [44]. The order of inhibition is decreased as the following order: 3>2>1.

Compound 3 is the most effective one due to: i) It has higher molecular weight ii) It contains 4N, O, S atoms which may act as adsorption centers and iii) it contains 4 hetero atoms. Compound 2 comes after compound 3 in inhibition efficiency due to: i) It contains 3N, 2O atoms and one Cl atom which is withdrawing group. This Cl atom enhances the electron density on the molecule and hence decreases the %IE and ii). It has lower molecular size and contains only two hetero atoms. Compound 1 is the least effective one due to: i) It has 2N, 2O, and one Cl atoms and ii) It has the least molecular size and contains one hetero atom.

CONCLUSION

1-The studied compounds have a great inhibition effect according to chemical type inhibitors for C-steel dissolution in 1.0M HCl solutions.

2-Reasonably good agreement was obtained between the values observed by the weight loss and electrochemical determinations were in good agreement. The order of %IE of these investigated compounds is in the following order: 3 > 2 > 1

3-The results obtained showed that the inhibition efficiency rises with inhibitor concentration and also increases with raising temperature.

4-Thermodynamic variables showed that the corrosion inhibition by studied inhibitors is owing to the chemical adsorbed film formation on the metal surface.

5-The inhibitor adsorption on C-steel surface in 1.0M HCl solution obeys Langmuir model for these inhibitors.

6-The negative signs of ΔG_{ads}^0 show spontaneous process of the inhibitors on the surface of C-steel.

7-The results of inhibition efficiency obtained from three techniques showed validity in results.

REFERNCES

- [1] A.A. El-Agamy, S.R. El-Gogary, R.T. Shalof, *Alex. J. Pharm. Sci.*, **2011**, 25, 2.
- [2] G. Trabanelli, *inhibitors - an old remedy for a new challenge Corrosion*, **1991**, 47, 410.
- [3] D. N. Singh, A. K. Dey, *Corrosion*, **1993**, 49, 594.
- [4] G. Banerjee, S.N., Malhotra, *UV and Raman spectroscopy Corrosion-NACE*, **1992**, 48, 10.
- [5] S. T. Arab, E. A. Noor, *Corrosion*, **1993**, 49, 122.
- [6] I. A. Raspini, *Corrosion*, **1993**, 49, 821.
- [7] N. Hajjaji, I. Ricco, A. Srhiri, A. Lattes, M. Soufiaoui, A. Benbachir, *Corrosion*, **1993**, 49, 326.
- [8] M. Elachouri, M. S. Hajji, M. Salem, S. Kertit, R. Coudert, E. M. Essassi, *Corros. Sci.*, **1995**, 37, 381.
- [9] H. Luo, Y. C. Guan, K. N. Han, *Corrosion*, **1998**, 54, 619.
- [10] M. A. Migahed, E. M. S. Azzam, A. M. Al-Sabagh, *Mater. Chem. Phys.*, **2004**, 85, 273.
- [11] M. M. Osman, A. M. Omar, A. M. Al-Sabagh, *Mater. Chem. Phys.*, **1997**, 50, 271.
- [12] F. Zucchi, G. Trabanelli, G. Brunoro, *Corros. Sci.*, **1992**, 33, 1135.
- [13] R.F. V. Villamil, P. Corio, J. C. Rubim, M. L. Siliva Agostinho, *J. Electroanal. Chem.*, **1999**, 472, 112.
- [14] T. P. Zhao, G. N. Mu, *Corros. Sci.*, **1999**, 41, 1937.
- [15] S. S. Abd El Rehim, H. Hassan., M. A. Amin, *Mater. Chem. Phys.*, **2001**, 70, 64.
- [16] S. S. Abd El Rehim, H. Hassan., M. A. Amin, *Mater. Chem. Phys.*, **2003**, 78, 337.
- [17] R. Guo T. Liu, X. Wei, *Colloids Surf. A*, **2002**, 37, 209.
- [18] V. Branzoi, F. Gologovici, F. Branzoi, *Mater. Chem. Phys.*, **2002**, 78, 122.
- [19] F. B. Traisnel, M. Lagrenee, *Corros. Sci.*, **2000**, 42, 127.
- [20] M.A. B. Christopher, A.R. G. Jenny, *Corros. Sci.*, **1994**, 36, 915.
- [21] M. Elachouri, M. S., Hajji, M. Salem, S. Kertit, J. Aride, R. Coudert, E. Essassi, *Corrosion*, **1996**, 52, 103.
- [22] A.S., Algaber, E.M., El-Nemma, M.M., Saleh, *Mater. Chem. Phys.* **2004**, 86, 26
- [23] D. J. Loren, F. Mansfeld, *Corros. Sci.*, **1981**, 21, 647.
- [24] S. S. Abdel-Rehim, K.F. Khaled, N. S. Abd-Elshafi, *Electrochim Acta*, **2006**, 51, 3269.
- [25] A.K., Maayta, N. A. F., *Al-Rawashdeh, Corros. Sci.*, **2004**, 46, 1129
- [26] A. V. Benedetti, P. T. A. Sumodjo, K. Nobe, P. L. Cabot, W. G. Proud, *Electrochim. Acta*, **1995**, 40, 2657.
- [27] E. M. Cafferty, N. Hackerman, *J. Electrochem Soc.*, **1972**, 119, 999.
- [28] J. Aljourani, K. Raeissi, M. A. Golozar, *Corros. Sci.*, **2009**, 51, 1836.
- [29] A. N. Wiercinska, G. Damata, *Electrochim. Acta*, **2006**, 51, 6179.
- [30] M. Kaminska, Z. Szklarska-Smialowska, *Corros. Sci.*, **1975**, 13, 557.
- [31] F. Bentiss, M. Traisnel, M. Lagrenee, *Corros. Sci.*, **2000**, 42, 127.
- [32] E. A. Noor. *Int. J. Electrochem. Sci.*, **2007**, 2, 996.
- [33] A. Y. Mousa, A. H. Kadhum, A. B. Mohamad, A. R. Daud, M. S. Takriff, S. K. Kamarudin, *Corros. Sci.*, **2009**, 51, 2393.
- [34] S. S. Abd El-Rehim., H. H. Hassan and M. A. Amin., *Mater. Chem. Phys.*, **2001**, 70, 64.
- [35] L. Tang, X. Lie, Y. Si, G. Mu and G. Liu, *Mater. Chem. Phys.*, **2006**, 95, 29-59.
- [36] G. Mu, X. Li, G. Liu, *Corros. Sci.*, **2005**, 47, 1932.
- [37] P. W. Atkins, *Physical Chemistry*, Fifthed, Oxford university press, **1994**, 877.
- [38] W. A. Badawy, K. M. Ismail, A. M. Fathi, *J. of Alloy and Comp.*, **2009**, 484, 365.
- [39] M.M. Solomon, S.A. Umoren, I. I. Udoso, A.P. Udoh, *Corros. Sci.*, **2010**, 52, 1317.
- [40] S. S. Abd El-Rehim, H. H. Hassan, M.A. Amin, *Mater. Chem. Phys.*, **2001**, 70, 64.
- [41] L. Tang, X. Lie, Y. Si, G. Mu, G. Liu, *Mater. Chem. Phys.*, **2006**, 95, 29.
- [42] G. Mu, X. Li, G. Liu, *Corros. Sci.*, **2005**, 47, 1932.

[43] S. Rajendran, *J. Electrochem. Soc.*,**2005**, 54,2, A.

[44] A.S. Fouda, M.M. Moussa, F.I.Taha, A.I. El-Neanaa, *Corros. Sci.*,**1986**, 26,719.